OPEN ACCESS
IOP Publishing
Journal of Physics A: Mathematical and Theoretical
J. Phys. A: Math. Theor. **53** (2020) 415201 (21pp)
https://doi.org/10.1088/1751-8121/abad77

Classical and quantum complex Hamiltonian curl forces

M V Berry

H H Wills Physics Laboratory, Tyndall Avenue, Bristol BS8 1TL, United Kingdom

Received 23 June 2020, revised 29 July 2020
Accepted for publication 7 August 2020
Published 10 September 2020

Abstract

A class of Newtonian forces, determining the acceleration $\boldsymbol{F}(x, y)$ of particles in the plane, is $\boldsymbol{F}$=(Re $F(z)$, Im $F(z)$), where z is the complex variable $x + \mathrm{i}y$. Curl $\boldsymbol{F}$ is non-zero, so these forces are nonconservative. These complex curl forces correspond to completely integrable Hamiltonians that are anisotropic in the momenta, separable in z and z^* but not in x and y if the curl is nonzero. The Hamiltonians can be quantised, leading to unfamiliar wavefunctions, even for the (non-curl) isotropic harmonic oscillator. The formalism provides an alternative interpretation of the analytic continuation of one-dimensional real Hamiltonian particle dynamics, where trajectories are known to exhibit intricate structure (though not chaos), and is a Hermitian alternative to non-Hermitian quantisation.

Keywords: non-Hermitian, PT symmetry, integrable

(Some figures may appear in colour only in the online journal)

1. Introduction

Curl forces [1] are Newtonian forces describing accelerations of particles. They depend on position (but not velocity), and are not the gradient of a potential, so their curl is not zero:

$$\ddot{\boldsymbol{r}} = \boldsymbol{F}(\mathbf{r}), \quad \nabla \times \boldsymbol{F} \neq 0. \tag{1.1}$$

These forces are non-conservative, because the work $\oint \mathrm{d}\mathbf{r} \cdot \boldsymbol{F}(\mathbf{r})$ done while transporting the particle around a circuit is non-zero, and equal to the flux of $\nabla \times \boldsymbol{F}$ through the circuit; nevertheless, they are non-dissipative, because volume in the state space of position and velocity is conserved. For most curl forces, there is no associated Hamiltonian or Lagrangian, and therefore no straightforward quantisation. But for a zero-measure subset of curl forces an underlying

Original content from this work may be used under the terms of the Creative Commons Attribution 4.0 licence. Any further distribution of this work must maintain attribution to the author(s) and the title of the work, journal citation and DOI.

Hamiltonian does exist [2, 3] and can be quantised. In such Hamiltonians, which may or may not be integrable [4], the kinetic energy is anisotropic in the canonical momenta.

My purpose here is to explore a subset of this Hamiltonian subset of curl forces, and their quantisation. These forces are characterised by an underlying complex structure. They describe a particle moving in the plane $\boldsymbol{r} = (x, y)$, and $\boldsymbol{F}(\boldsymbol{r})$ depends only on the complex variable $z = x + \mathrm{i}y$ through a scalar function $F(z)$. For such 'complex curl forces', (1.1) reduces to dynamics in the complex plane:

$$\ddot{z} = F(z), \quad (z = x + \mathrm{i}y). \tag{1.2}$$

The function $F(z)$ is assumed to be analytic in the z plane, possibly with isolated pole or branch-point singularities.

Complex classical dynamics of this type has been extensively studied from a different viewpoint [5]. Starting from the one-dimensional Hamiltonian

$$H(x, p) = \frac{1}{2}p^2 + U(x), \tag{1.3}$$

with real x, p, in which $U(x, y)$ need not be real, the variable x has been extended to the complex plane. A series of remarkable researches [6–11] has revealed that even for simple potentials $U(z)$ the solutions of (1.2) represent exquisitely intricate trajectories.

The additional perspectives provided here are that the complex dynamics (1.2) has the following features: it represents a special case of curl force dynamics; it is generated in the real plane x, y by a real and completely integrable two-freedom real Hamiltonian; and it can be quantised in the real plane. Section 2 describes the classical Hamiltonian, using two different representations, one of which is separable for any curl force $F(z)$. Section 3 describes the corresponding Hermitian quantisation. Section 4 explores some examples; although simple, these possess unanticipated subtle features. This study raises questions that point to directions for further study; some are listed in the concluding section 5.

We are here considering real x and y and also real t, but note that when t is complexified the dynamics has additional richness. One motivation for this is the motion of electrons in crystals when a magnetic field is applied [12]. Then the force depends on velocity as well as position, but the dynamics (1.2) is still relevant because the velocity dependence can sometimes be eliminated by transforming to a complex time variable that may be periodic [13] as a function of physical (real) time. The associated return maps display intricate fractal structure [14].

To avoid possible confusions, I note that the class of curl forces (1.2) is different from the curl force (a.k.a. 'scattering force') exerted on a small polarisable absorbing particle by an optical field $\psi(\boldsymbol{r})$ [3, 15], even when this is has the form $\psi(x + \mathrm{i}y)$. This optical force is $\boldsymbol{F}(\mathbf{r}) = \mathrm{Im}\,[\psi^*(\mathbf{r})\,\nabla\psi(\mathbf{r})]$, which is different from (1.2) except for the case of a single optical vortex, for which $\psi = x + \mathrm{i}y$ and $F(z) = \mathrm{i}z$ in (1.2). Second, I will not discuss non-Hermitian quantisation, with its focus on PT symmetry, about which great deal is already known [16].

2. Classical Hamiltonian curl force formalism

It is easy to check that for the complex dynamics (1.2) the curl vector in (1.1) is

$$(\nabla \times \boldsymbol{F})_\perp \equiv C(\mathbf{r}) = 2\ \mathrm{Im}\ F'(z), \tag{2.1}$$

so all these complex forces have non-zero curl, except for the trivial case $F(z) = \pm z + \text{constant}$.

To display the Hamiltonian structure underlying (1.2), the first step is to define the natural 'potential', satisfying Laplace's equation,

$$F(z) = -U'(z), \quad \text{i.e.} U(z) = -\int_0^z \mathrm{d}\zeta F(\zeta). \tag{2.2}$$

Then (1.2) implies the complex conserved 'energy'

$$\frac{1}{2}\dot{z}^2 + U(z) = E_\mathrm{c}, \tag{2.3}$$

which determines the velocity (up to a sign representing time-reversal); it follows that trajectories with the same E_c cannot cross [6].
The trajectories $z(t)$ for any $U(z)$ and specified E_c are the integral curves of the velocity vector $\mathbf{v} = \{\mathrm{Re}\ \dot{z}, \mathrm{Im}\ \dot{z}\}$, and can be obtained formally by quadrature:

$$t - t_0 = \int_{z_0}^{z(t)} \frac{\mathrm{d}z}{\sqrt{2\,(E_\mathrm{c} - U(z))}}. \tag{2.4}$$

This conceals more than it reveals, because of the complications introduced by the Riemann surface structure [14] associated with the branch cuts and inverse functions required to determine the trajectory. An important role is played by the stagnation points [6] defined by $U(z) = E_\mathrm{c}$, where the velocity vanishes.

The real and imaginary parts of E_c correspond to two real conserved quantities:

$$\frac{1}{2}\left(\dot{x}^2 - \dot{y}^2\right) + \mathrm{Re}\ U(x+\mathrm{i}y) = E, \quad \dot{x}\dot{y} + \mathrm{Im}\ U(x+\mathrm{i}y) = K \tag{2.5}$$

either can be defined as a Hamiltonian generating (1.2). We choose the Hamiltonian corresponding to the first conservation law:

$$H = E = \frac{1}{2}\left(p_x^2 - p_y^2\right) + \mathrm{Re}\ U(x+\mathrm{i}y), \quad \text{i.e.}\ p_x = \dot{x}, \quad p_y = -\dot{y}. \tag{2.6}$$

The second conservation law then corresponds to the additional conserved phase-space function

$$-p_x p_y + \mathrm{Im}\ U(x+\mathrm{i}y) = K. \tag{2.7}$$

(The alternative Hamiltonian defined by the second conserved quantity in (2.5) is $+p_x p_y + \mathrm{Im}\ U(x+\mathrm{i}y)$, and the association between velocities and momenta is different: $\dot{x} = p_y, \dot{y} = p_x$.) The existence of a second integral of motion implies that the Hamiltonian (2.6) (or (2.7)) is completely integrable (though usually nonseparable) [14]: therefore in the dynamics (1.2), there is no chaos. (The anisotropic Kepler problem [17, 18], describing electrons in semiconductors and familiar in quantum chaology, is an example of a Hamiltonian curl force [2]; but it does not belong to the class (2.6) because its potential $U(x, y) = -1/\sqrt{(x^2 + y^2)}$ is not the real part of a function of $x + \mathrm{i}y$; moreover it is nonintegrable.)

To prepare for quantisation, it is convenient to express the Hamiltonian (2.6) in terms of new phase space variables, with coordinates z and z^*, regarded as independent coordinates, and the convenient notation

$$\begin{aligned} X = z = (x+\mathrm{i}y), \ Y = z^* = (x-\mathrm{i}y), \\ P_X = \frac{1}{2}\left(p_x - \mathrm{i}p_y\right), \ P_Y = \frac{1}{2}\left(p_x + \mathrm{i}p_y\right). \end{aligned} \tag{2.8}$$

Then (2.6) becomes the alternative Hamiltonian

$$H = \left(P_X^2 + \frac{1}{2}U(X)\right) + \left(P_Y^2 + \frac{1}{2}U^*(Y)\right) = E = E_X + E_Y, \tag{2.9}$$

which is obviously separable, with energies E_X, E_Y corresponding to the two freedoms in this representation. The second conserved quantity (2.7) transforms to

$$\mathrm{i}K = \left(P_X^2 + \frac{1}{2}U(X)\right) - \left(P_Y^2 + \frac{1}{2}U^*(Y)\right) = +(E_X - E_Y), \tag{2.10}$$

which is simply an awkward way of stating that the X and Y Hamiltonians are conserved separately. It is worth emphasising that this complexification is different from the more familiar procedure in which coordinates and momenta are mixed [19].

3. Quantum complex curl force formalism

The Hamiltonian (2.6) can be quantised in the familiar way, using $p_x = -\mathrm{i}\partial_x$, $p_y = -\mathrm{i}\partial_y$, leading to a Schrödinger equation involving a Hermitian operator:

$$\left(\left(-\partial_x^2 + \partial_y^2\right) + \frac{1}{2}\ \mathrm{Re}\ U(x + \mathrm{i}y)\right)\psi(\mathbf{r}) = E\psi(\mathbf{r}). \tag{3.1}$$

The different signs in the x and y derivatives are a characteristic feature of complex curl force quantisation, and will have unexpected consequences. With the exception of the free particle and linear potential, to be considered in sections 4.1 and 4.2, the potential $\mathrm{Re}\ U(x + \mathrm{i}y)$ is not separable in x and y.

However, the form (2.9) is separable, and the substitution $P_X = -\mathrm{i}\partial_X, P_Y = -\mathrm{i}\partial_Y$ leads to the Schrödinger equation

$$\left(-\partial_X^2 - \partial_Y^2 + \frac{1}{2}U(X) + \frac{1}{2}U^*(Y)\right)\Psi(X,Y) = (E_X + E_Y)\Psi(X,Y) = E\Psi(X,Y), \tag{3.2}$$

whose solution is any superposition of the product wavefunctions

$$\Psi(X,Y) = \Psi((x + \mathrm{i}y),(x - \mathrm{i}y)) = \psi_X(X)\psi_Y(Y), \tag{3.3}$$

where ψ_X and ψ_Y satisfy

$$\begin{aligned}\left(-\partial_X^2 + \frac{1}{2}U(X)\right)\psi_X(X) &= E_X\psi_X(X),\\ \left(-\partial_Y^2 + \frac{1}{2}U^*(Y)\right)\psi_Y(Y) &= E_Y\psi_Y(Y).\end{aligned} \tag{3.4}$$

It is easy to check directly that $\Psi(\boldsymbol{r}) = \Psi(X(x,y), Y(x,y))$ is a solution of (3.1). Thus is established the quantisation of the classical complex curl forces defined by (1.2). The energy is $E = E_X + E_Y$. We will mostly consider E real; E_X and E_Y need not be real, and then $\mathrm{Im}\ E_X = -\mathrm{Im}\ E_Y$ can be interpreted as ψ_X describing gain or loss, with ψ_Y describing a compensating loss or gain.

The complex-separated Hamiltonian in (3.2) is Hermitian, but the separate X and Y contributions in (3.4) are non-Hermitian Hamiltonians. The separate Schrödinger equations in (3.4), are the same as the analytically continued one-dimensional operators studied in non-Hermitian

quantum mechanics [16]. These studies, particularly where $U(X)$ is non-Hermitian and PT symmetric, have led to ingenious interpretations, involving waves decaying in particular sectors of the x, y plane, leading to a discrete spectrum of real energies. Here the different focus is on dynamics and quantisation of curl forces in the full real x, y plane.

4. Simple examples

4.1. Free particle

When $U(z) = 0$, the solutions of (3.1) are

$$\psi(x,y) = \exp\left(\mathrm{i}\left(k_x x + k_y y\right)\right), \quad E = \frac{1}{2}\left(k_x^2 - k_y^2\right), \tag{4.1}$$

which are propagating plane waves for k_x and k_y real. The solutions of (3.2) in the separated form (3.3) are

$$\begin{gathered}\Psi(X,Y) = \exp\left(\mathrm{i}\left(K_X X + K_Y Y\right)\right) = \exp\left(\mathrm{i}\left(K_X + K_Y\right)x\right)\exp\left(\left(K_Y - K_X\right)y\right), \\ E = K_X^2 + K_Y^2.\end{gathered} \tag{4.2}$$

which are evanescent or growing waves for K_X and K_Y real. To recapture the propagating plane waves (4.1), it is necessary to choose separated momenta that are complex (cf (2.8)):

$$K_X = \frac{1}{2}\left(k_x - \mathrm{i}k_y\right), \quad K_Y = \frac{1}{2}\left(k_x + \mathrm{i}k_y\right). \tag{4.3}$$

Perhaps surprisingly, evanescent plane waves (K_X, K_X real), can be expressed as superpositions of propagating waves (k_X, k_X real) [20]; extensions of this idea will be used in the next two sections.

4.2. Linear potential

This is

$$U(z) = az, \quad (a = a_1 + ia_2), \quad \text{i.e.} \quad \mathrm{Re}\, U(x + \mathrm{i}y) = a_1 x - a_2 y, \tag{4.4}$$

which according to (1.2) and (2.2), corresponds to the constant force $F = -a$, i.e. force vector $\boldsymbol{F} = (-a_1, -a_2)$. For positive a_1, a_2, particles in the positive quadrant $x > 0$, $y > 0$ are attracted to the x and y axes. This simple example is not a curl force (cf (2.1)), because the force is constant; nevertheless it is instructive to examine it in some detail.

The Schrödinger equation (3.1) is

$$\left(\frac{1}{2}\left(-\partial_x^2 + \partial_y^2\right) + a_1 x - a_2 y\right)\psi(\mathbf{r}) = E\psi(\mathbf{r}). \tag{4.5}$$

This special case is separable in x, y for all a, and general solutions with energy E involve superpositions of linear combinations $C\mathrm{i}_1$, $C\mathrm{i}_2$ of the Airy functions $A\mathrm{i}$ and $B\mathrm{i}$ [21]:

$$\begin{gathered}\psi(x,y) = C\mathrm{i}_1\left((2a_1)^{1/3}\left(x - \frac{E_x}{a_1}\right)\right) C\mathrm{i}_2\left((2a_2)^{1/3}\left(y - \frac{E_y}{a_2}\right)\right), \\ E = E_x - E_y.\end{gathered} \tag{4.6}$$

For fixed E, this is a one-parameter family of degenerate states, labelled by E_x or E_y.

An unsurprising special case is the orthonormal eigenfunctions in the positive quadrant, decaying at infinity and with Dirichlet boundary conditions on the axes, namely

$$\begin{aligned}\psi_{m,n}(\mathbf{r}) &= \left(\frac{4}{a_1 a_2}\right)^{1/6} \frac{\mathrm{Ai}\left((2a_1)^{1/3}x-\alpha_m\right)\mathrm{Ai}\left((2a_2)^{1/3}y-\alpha_n\right)}{\mathrm{Ai}'(-\alpha_m)\,\mathrm{Ai}'(-\alpha_n)},\\ \{m,n\} &= 1,2,3\ldots, E_{m,n} = \frac{1}{2^{1/3}}\left(\alpha_n a_2^{2/3}-\alpha_m a_1^{2/3}\right),\end{aligned} \tag{4.7}$$

in which the positive numbers α_n are the Airy zeros: $\mathrm{Ai}(-\alpha_n)=0$. The mode energies $E_{m,n}$ are negative as well as positive (because of the signs in the derivatives in (3.1)), and real and nondegenerate for almost all a_1, a_2 (if $a_1=a_2$, $E=0$ is infinitely degenerate, and if a_1 and a_2 are proportional to Airy zeros some levels are pairwise degenerate). Figure 1(a) illustrates one of these modes. The corresponding classical trajectory (figure 1(b)) consists of segments of parabolas with accelerations $-a_1$, $-a_2$, specularly reflected from the axes, and bounded by a rectangular caustic. This is standard torus quantisation of an integrable quantum system.

For the general complex-separated form (3.3), the functions ψ_X and ψ_Y in the product wavefunction $\Psi(X,Y)$ can alternatively be expressed in terms of any linear combinations $C\mathrm{i}$ of $A\mathrm{i}$ and $B\mathrm{i}$:

$$\begin{aligned}\psi_X(X) &= C\mathrm{i}_1\left(\left(X-\frac{2E_X}{a}\right)\left(\frac{1}{2}a\right)^{1/3}\right)+C\mathrm{i}_2\left(\left(X-\frac{2E_X}{a}\right)\left(\frac{1}{2}a\right)^{1/3}\right),\\ \psi_Y(Y) &= C\mathrm{i}_3\left(\left(Y-\frac{2E_Y}{a^*}\right)\left(\frac{1}{2}a^*\right)^{1/3}\right)+C\mathrm{i}_3\left(\left(Y-\frac{2E_Y}{a^*}\right)\left(\frac{1}{2}a^*\right)^{1/3}\right),\\ E &= E_X+E_Y.\end{aligned} \tag{4.8}$$

Here we encounter the first unfamiliar feature: these X, Y complex-separated states are very different from those of the x, y real separation (4.6). This is illustrated in figure 1(c) for the case where the $C\mathrm{i}_1$ and $C\mathrm{i}_3$ are $A\mathrm{i}$ functions and $C\mathrm{i}_2=C\mathrm{i}_4=0$ (i.e. Ψ is the product of two Airy functions), for the same a and E and the same quadrant as $\psi_{m,n}$ in figure 1(a). The two lines of isolated zeros correspond to points where the argument of each of the two $A\mathrm{i}$ functions is real and equal to any of the Airy zeros $-\alpha_n$, contrasting with the intersecting line zeros of the real modes $\psi_{m,n}$. The asymptotics of $A\mathrm{i}$ and $B\mathrm{i}$ [21], in particular the Stokes phenomenon [22], imply, in contrast to the exponential decay of the modes $\psi_{m,n}$ in the positive quadrant, that for all choices of the $C\mathrm{i}_1\ldots C\mathrm{i}_4$ there are sectors in each quadrant of the x, y plane where Ψ diverges exponentially [e.g. as $\mathrm{O}(\exp(|\boldsymbol{r}|^{3/2}))$] (see figure 1(c) where the wave rises to $\sim\mathrm{e}^{40}$ on the edge of the region shown).

The two separations must be related, because both families of states are solutions of (4.5). To illustrate the relation, we choose superpositions of the standard $A\mathrm{i}$ functions, and for convenience write the wavefunctions using Dirac state-vector notation. For (4.6), this is

$$\begin{aligned}\left\langle \mathbf{r}\,\middle|\,\psi\left(E_x,E_y\right)\right\rangle &= \frac{2^{2/3}}{(a_1a_2)^{1/6}}\mathrm{Ai}\left((2a_1)^{1/3}\left(x-\frac{E_x}{a_1}\right)\right)\mathrm{Ai}_2\left((2a_2)^{1/3}\left(y-\frac{E_y}{a_2}\right)\right),\\ E &= E_x-E_y.\end{aligned} \tag{4.9}$$

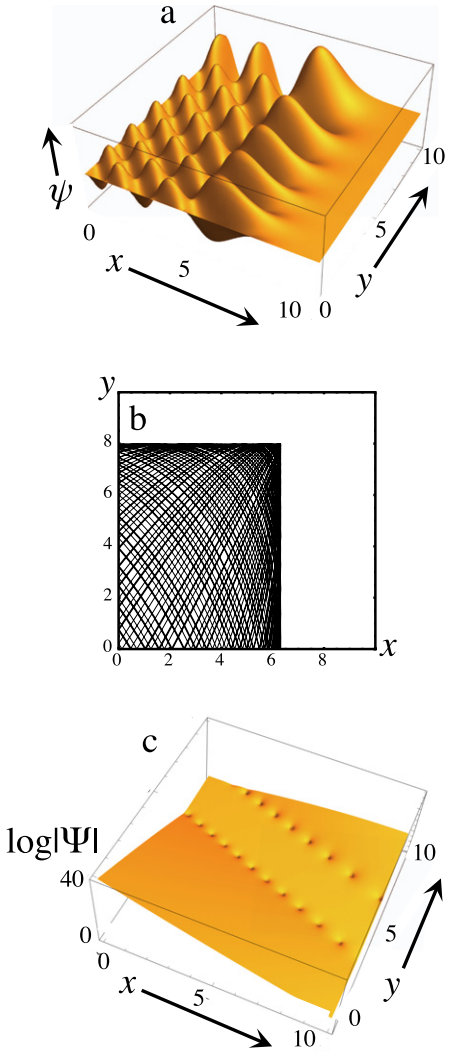

Figure 1. (a) Mode $\psi_{5,10}(\boldsymbol{r})$ in (4.7), for $a = 1 + 2\mathrm{i}$. (b) The corresponding classical trajectory, (c) complex-separated mode $\log|\Psi|$ in (4.8) with $C\mathrm{i} = A\mathrm{i}$, also with $a = 1 + 2\mathrm{i}$, and $E_X = 15\mathrm{i}$, $E_Y = 5{-}15\mathrm{i}$.

States with different E_x, E_y are orthogonal, and the prefactor ensures the normalisation

$$\left\langle \psi\left(E_{1x}, E_{1y}\right) \middle| \psi\left(E_{2x}, E_{2y}\right)\right\rangle = \delta\left(E_{1x} - E_{2x}\right)\delta\left(E_{1y} - E_{2y}\right). \tag{4.10}$$

This follows from [23]

$$\int_{-\infty}^{\infty} \mathrm{d}\xi\ A\mathrm{i}\left(\xi - c\right)A\mathrm{i}\left(\xi - d\right) = \delta\left(c - d\right). \tag{4.11}$$

The states (4.9) are not square-integrable in the full x, y plane, but they are bounded everywhere. The unbounded corresponding complex-separated states (cf (4.8) are

$$\begin{aligned}&\left\langle \mathbf{r}\,\middle|\,\Psi\left(E_X,E_Y\right)\right\rangle\\&\quad=A\mathrm{i}\left(\left(\frac{1}{2}a\right)^{1/3}\left((x+\mathrm{i}y)-\frac{2E_X}{a}\right)\right)A\mathrm{i}\left(\left(\frac{1}{2}a^*\right)^{1/3}\left(x-\mathrm{i}y-\frac{2E_Y}{a^*}\right)\right),\\&E=E_X+E_Y\cdot\end{aligned}\tag{4.12}$$

Note the different signs in the energies in (4.9) and (4.12).

The relation between the two separations is that each of the states $|\Psi\rangle$ in (4.12) can be written as a superposition of the states $|\psi\rangle$ in (4.9):

$$\left|\Psi\left(E_X,E_Y\right)\right\rangle=\iint \mathrm{d}E_x\ \mathrm{d}E_y\left\langle\psi\left(E_x,E_y\right)\,\middle|\,\Psi\left(E_X,E_Y\right)\right\rangle\left|\psi\left(E_x,E_y\right)\right\rangle.\tag{4.13}$$

The overlap, derived in appendix A, is

$$\begin{aligned}&\left\langle\psi\left(E_x,E_y\right)\,\middle|\,\Psi\left(E_X,E_Y\right)\right\rangle\\&\quad=\frac{1}{\left(a_1a_2\right)^{1/6}}A\mathrm{i}\left(-\frac{2^{1/6}}{\left(|a|^2a_1a_2\right)^{2/3}}\left(a_2^2E_x+a_1^2E_y+\mathrm{i}a_1a_2\left(E_X-E_Y\right)\right)\right)\\&\qquad\times\delta\left(E_X+E_Y-E_x+E_y\right).\end{aligned}\tag{4.14}$$

The δ function confirms that any of the degenerate states $|\Psi\rangle$ with energy E can be expressed as a superposition of the degenerate states $|\psi\rangle$ with the same energy E.

The superposition relating the separations could equally be carried out in the positive quadrant rather than the full x, y plane, with Ψ expressed as a sum over the discrete states $\psi_{m,n}$ in (4.7). Although $\psi_{m,n}$ satisfies Dirichlet boundary conditions, Ψ does not. At the classical level, this corresponds to Ψ being the quantisation of a collection of trajectories of the torus type in figure 1(b), exploring rectangles of different side ratios.

It is worth remarking that for linear potentials the separations (4.9) and (4.12) are two members of a more general family, all satisfying (4.5):

$$\begin{aligned}\Psi\left(x,y;A,B\right)=A\mathrm{i}&\left((Ax+By)\left(\frac{2\left(Aa_1+Ba_2\right)}{\left(B^2-A^2\right)^2}\right)^{1/3}-E_1\left(\frac{2\left(A^2-B^2\right)}{\left(Aa_1+Ba_2\right)^2}\right)^{1/3}\right)\\&\times A\mathrm{i}\left((Bx+Ay)\left(\frac{2\left(Aa_2+Ba_1\right)}{\left(B^2-A^2\right)^2}\right)^{1/3}-E_2\left(\frac{2\left(A^2-B^2\right)}{\left(Aa_2+Ba_1\right)^2}\right)^{1/3}\right),\end{aligned}\tag{4.15}$$

with energy $E=E_1$–E_2. The separation (4.9) corresponds to $A=1$, $B=0$, and (4.12) corresponds to $A=1$, $B=\mathrm{i}$.

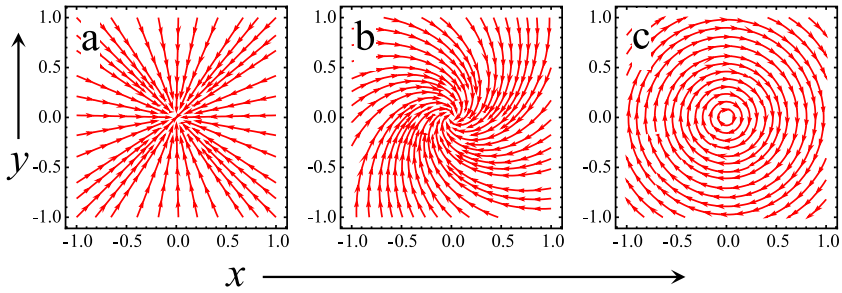

Figure 2. Force vectors and their integral curves for the quadratic potential (linear force) (4.16), for (a) $a = 1$ (not a curl force), (b) $a = \sqrt{i}$, (c) $a = \mathrm{i}$.

4.3. Quadratic potential

The classical trajectories for this simple case were understood in detail in the context of complex dynamics [24] and also for curl forces [3, 15], so a brief description will suffice. The potential and dynamics are

$$U(z) = \frac{1}{2}az^2 \Rightarrow \ddot{z} = -az, \tag{4.16}$$

in which $a = a_1 + \mathrm{i}a_2$ can be any complex number. Complex curl forces correspond to $a_2 \neq 0$, i.e. $\arg a \neq (0, \pi)$, and, from (2.1), the curl of the force vector is constant:

$$C(\mathbf{r}) = -2a_2. \tag{4.17}$$

The general solution is

$$z(t) = A_+ \ \exp\left(\mathrm{i}t\sqrt{a}\right) + A_- \ \exp\left(-\mathrm{i}t\sqrt{a}\right). \tag{4.18}$$

with different orbits labelled by the complex numbers A_+ and A_-. Multiplying A_+ and A_- by a common complex factor rotates and magnifies the trajectory, and changing $|a|$ rescales t. The complex conserved 'energy' (2.3) is

$$E_\mathrm{c} = 2aA_+A_-. \tag{4.19}$$

As illustrated in figure 2, the force vectors depend qualitatively on $\arg a$. The vectors spiral into the origin (attracting) if $-\frac{1}{2}\pi < \arg\ a\,(\mathrm{mod}\ \ 2\pi) < \frac{1}{2}\pi$, and spiral out (repelling) otherwise.

Positive real a (figure 2(a)) is not a curl force, and corresponds to the equal-frequency harmonic oscillator (SHO), all of whose orbits are periodic and elliptical. For all other values of a, orbits are unbounded. For attracting a with $a_2 \neq 0$—that is, for curl forces—the orbits spiral in from infinity, loop around the zero-velocity stagnation points while reversing their curvature, and then spiral out to infinity. This influence of the stagnation points is a well-understood general feature of complex dynamics [25]. For repelling a, the orbits curve in from infinity and out to infinity without spiralling. Imaginary a (figure 2(c)) is the pure curl case, previously considered [1] as a force with rotational symmetry. Angular momentum is not conserved for these curl forces, because there is an angular torque; this does not violate Noether's theorem because the negative sign in the kinetic energy in (2.6) means that the Hamiltonian does not possess rotational symmetry: angular momentum is not an invariant in this case. Figure 3 shows

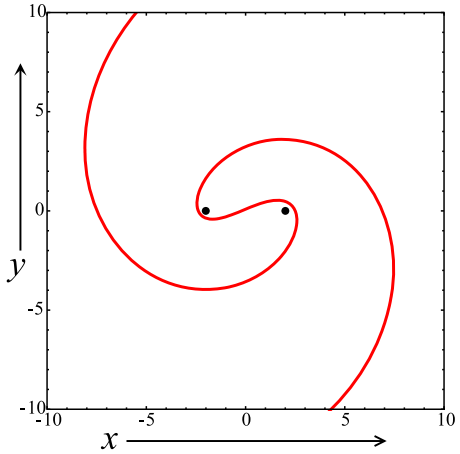

Figure 3. Complex orbit (4.18) under the linear curl force (4.16), for $a = 1 + \mathrm{i}$, $A_+ = 1/A_- = 0.5$; the black dots are the stagnation points, around which the orbit winds after approaching and before receding.

a typical example of a spiralling trajectory, driven by a force that spirals into the origin as in figure 2(b).

The Schrödinger equation (3.1) is

$$\left(\frac{1}{2}\left(-\partial_x^2+\partial_y^2\right)+\frac{1}{2}a_1\left(x^2-y^2\right)-a_2xy\right)\psi\left(\boldsymbol{r}\right)=E\psi\left(\boldsymbol{r}\right). \tag{4.20}$$

The potential possesses a saddle at $\boldsymbol{r}=0$, and two collinear valleys, orthogonal to which are two barriers; changing a_1 and a_2 simply rotates this structure. This Schrödinger equation is nonseparable in x and y for $a_2\neq 0$, that is, for curl forces, because of the negative sign in the kinetic energy. But from (3.3) and (3.4) it is separable in X and Y, with factor functions that are general solutions of (3.4), expressible as parabolic cylinder functions D [21]:

$$\psi_X\left(X\right)=C_1D_{-1/2+E_X/\sqrt{a}}\left(a^{1/4}X\right)+C_2D_{-1/2-E_X/\sqrt{a}}\left(\mathrm{i}a^{1/4}X\right), \tag{4.21}$$

and similarly for ψ_Y. A convenient choice for the product solution is

$$\begin{aligned}\Psi\left(\mathbf{r},E_X,E_Y\right)=\left\langle\mathbf{r}\right|\left.\Psi\left(E_X,E_Y\right)\right\rangle=D_{-1/2+E_X/\sqrt{a}}\left(a^{1/4}\left(x+\mathrm{i}y\right)\right)\\ \times D_{-1/2+E_Y/\sqrt{a^*}}\left(\mathrm{i}a^{*1/4}\left(x-\mathrm{i}y\right)\right),\end{aligned} \tag{4.22}$$

with the sign of E_Y chosen so that the energy is

$$E=E_X-E_Y. \tag{4.23}$$

For all non-real a, that is, for all curl forces, the Stokes phenomenon [22] controlling the large-argument asymptotics of D [21] indicates that $\Psi(\boldsymbol{r},E_X,E_Y)$ grows exponentially towards infinity for some sectors in the x, y plane, for almost all E_X, E_Y. The choice (4.22) ensures that Ψ does not diverge exponentially for x, y in the positive quadrant when $0\leqslant\arg\ a<\pi/2$. This is because the product of the leading exponentials in the asymptotics of the two D factors has

modulus unity for all a: the product is a pure phase factor, with phase $-\frac{1}{2}\left(x^2-y^2\right)\mathrm{Im}\ \sqrt{a}-xy\ \mathrm{Re}\ \sqrt{a}$.

However, for E_X, E_Y for which the arguments of D are non-negative integers, the growth is power-law, rather than exponential, in all sectors of the x, y plane and for all a. For these particular solutions [21], D involves the Hermite polynomials H, and

$$\Psi_{m,n}(\mathbf{r}) = \left\langle \mathbf{r} \middle| \Psi_{m,n} \right\rangle = \frac{1}{2^{\frac{1}{2}(m+n)}}\ \exp\left(-\mathrm{i}\left(\frac{1}{2}\left(x^2-y^2\right)\mathrm{Im}\sqrt{a}+xy\ \mathrm{Re}\ \sqrt{a}\right)\right) \times H_n\left(\frac{a^{1/4}}{\sqrt{2}}(x+\mathrm{i}y)\right) H_m\left(\frac{a^{*1/4}}{\sqrt{2}}(\mathrm{i}x+y)\right), \tag{4.24}$$

This satisfies (4.19) with energy (complex for curl forces, i.e. $a_2 \neq 0$)

$$E_{m,n} = \sqrt{a}\left(m+\frac{1}{2}\right) - \sqrt{a^*}\left(n+\frac{1}{2}\right) \quad (m=0,1,2\ldots, n=0,1,2\ldots). \tag{4.25}$$

For $a_2 \neq 0$, the solutions (4.22), and the power-law growing modes (4.24), are quantum states corresponding to classical curl forces. The special case of quadratic potentials that do not generate curl forces, i.e. a positive real, corresponds to the isotropic SHO, with Schrödinger equation (4.20) that is separable in x and y. The familiar orthonormal eigenstates, written without loss of essential generality for $a=1$, are

$$\psi_{m,n}(\mathbf{r}) = \left\langle \mathbf{r} \middle| \psi_{m,n} \right\rangle = \frac{\exp\left(-\frac{1}{2}\left(x^2+y^2\right)\right)}{\sqrt{\pi m! n! 2^{m+n}}} H_m(x) H_n(y), \tag{4.26}$$

with energies

$$E_{m,n} = m-n. \tag{4.27}$$

Note the sign, which follows from the signs in (4.20). As a consequence, these states are infinitely degenerate in an unusual way:

$$E_{m,n} = E_{m+k,n+k}. \tag{4.28}$$

But for this case $a=1$ the complex-separated solutions (4.24) have exactly the same real energies (4.27), so, as for the linear potential, the question arises of the relation between the two sets of states. As figure 4 illustrates, the states look very different. The conventional SHO states $\psi_{m,n}$ in (4.26) (figures 4(a) and (b)) are real, and possess intersecting patterns of nodal lines associated with the zeros of the two Hermite polynomials. By contrast, the complex-separated states $\Psi_{m,n}$ (4.24) (figure 4(c)) possess isolated zeros along the x and y axes.

As with the linear potential, the relation is that any of the states $|\Psi_{m,n}\rangle$ can be reproduced by superposing the degenerate SHO states $|\psi_{m+k,n+k}\rangle$ with the same energy:

$$|\Psi_{m,n}\rangle = \sum_{k=0}^{\infty} c_{m,n,k} |\psi_{m+k,n+k}\rangle. \tag{4.29}$$

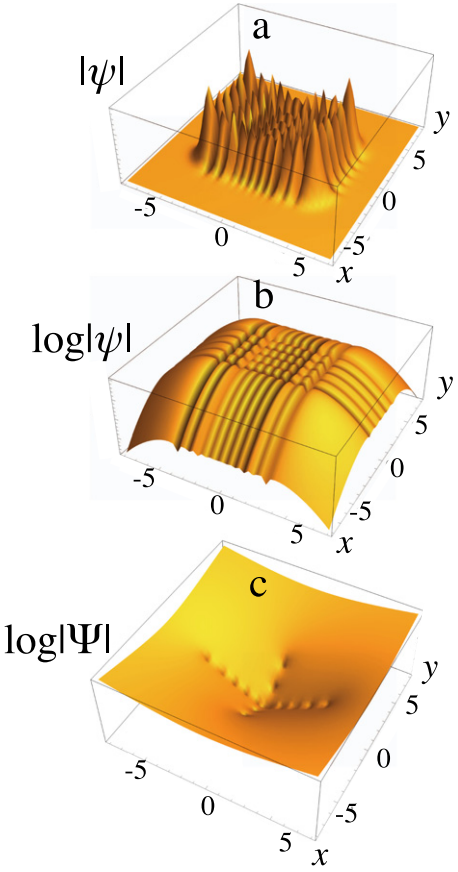

Figure 4. Quantum modes for the SHO, i.e. solutions of (4.20) with $a_2 = 0$, with quantum numbers $m = 10$, $n = 5$, so the energy is $E = 5$. (a) The classical Hermite–Gauss wave amplitude $|\psi_{10,5}(\boldsymbol{r})|$ (equation (4.26)); (b) the same state, plotted as $\log|\psi_{10,5}(\boldsymbol{r})|$; (c) the complex-separated mode $\log|\Psi_{10,5}(\boldsymbol{r})|$ (equation (4.24)).

The coefficients are

$$\begin{aligned} c_{m,n,k} &= \left\langle \psi_{m+k,n+k} \,\middle|\, \Psi_{m,n} \right\rangle \\ &= \frac{1}{\sqrt{\pi m!n!2^{m+n}}} \iint \mathrm{d}\boldsymbol{r}\ \exp\left(-\frac{1}{2}\left(x^2+y^2\right) - \mathrm{i}xy\right) \\ &\quad \times H_{m+k}(x)\, H_{n+k}(y)\, H_m\left(\frac{1}{\sqrt{2}}(x+\mathrm{i}y)\right) H_n\left(\frac{1}{\sqrt{2}}(\mathrm{i}x+y)\right). \end{aligned} \tag{4.30}$$

The double integral converges and can be evaluated explicitly for any values m, n, k. I do not have a general form, but the first few coefficients, with the convenient scaling

$$c_{m,n,k} \equiv \sqrt{2\pi}(-\mathrm{i})^k d_{m,n,k}, \quad k' = k+1, \tag{4.31}$$

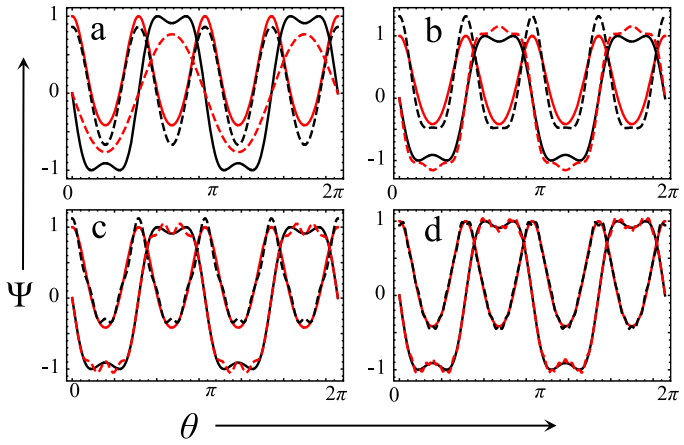

Figure 5. Approximations $\Psi_{K,0,0}(\boldsymbol{r})$ in (4.34) for the complex mode $\Psi_{0,0}(\boldsymbol{r})$ as a series of the SHO eigenmodes $\psi_{k,k}(\boldsymbol{r})$, around the circle $\boldsymbol{r} = (r\,\cos\,\theta,\, r\,\sin\,\theta)$ with $r = 2$, for (a) $K = 2$; (b) $K = 5$; (c) $K = 20$; (d) $K = 100$. Full red curves: $\mathrm{Re}\,(\Psi_{00}\,(\mathbf{r})) = \cos\left(\frac{1}{2}r^2\,\sin\,2\,\theta\right)$; full black curves: $\mathrm{Im}\,(\Psi_{00}\,(\mathbf{r})) = -\sin\left(\frac{1}{2}r^2\,\sin\,2\,\theta\right)$; dashed black curves: approximation $\mathrm{Re}(\Psi_{\kappa,00}(\boldsymbol{r}))$; dashed red curves: approximation $\mathrm{Im}(\Psi_{\kappa,00}(\boldsymbol{r}))$

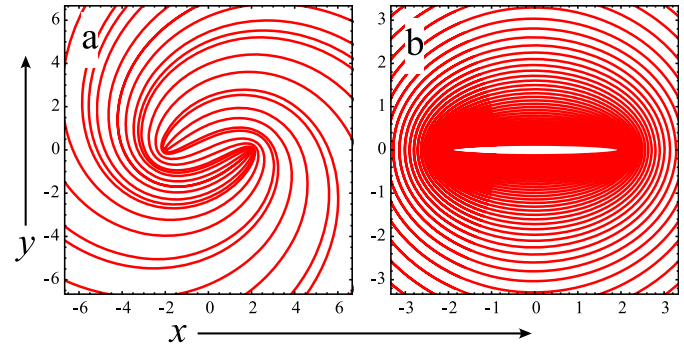

Figure 6. Families of classical trajectories with the same energy. (a) $a = \sqrt{(2i)}$, $E_c = 2\sqrt{(2i)}$, $A_+ = 0.1(0.1)1.0$, $A_- = 1/A_+$; (b) $a = 1/2$, $E = 1$, $A_+ = 0.1(0.02)0.95$, $A_- = 1/A_+$.

are

$$
\begin{aligned}
&d_{0,0,k} = 1, \quad d_{0,1,k} = 2\sqrt{k'}, \quad d_{1,1,k} = 2\left(2k'+1\right),\\
&d_{0,2,k} = 4\sqrt{k'^2+k'}, \quad d_{1,2,k} = 8\left(k'+1\right)\sqrt{k'+2}, \quad d_{2,2,k} = 8\left(2k'^2+6k'+5\right),\\
&d_{0,3,k} = 8\sqrt{k'^3+3k'^2+2k'}, \quad d_{1,3,k} = 8\sqrt{4k'^4+24k'^3+53k'^2+51k'+18},\\
&d_{2,3,k} = 162\left(k'^2+8k'+9\right)\sqrt{k'+2}, \quad d_{3,3,k} = 16\left(4k'^3+30k'^2+8k'+75\right).
\end{aligned}
\tag{4.32}
$$

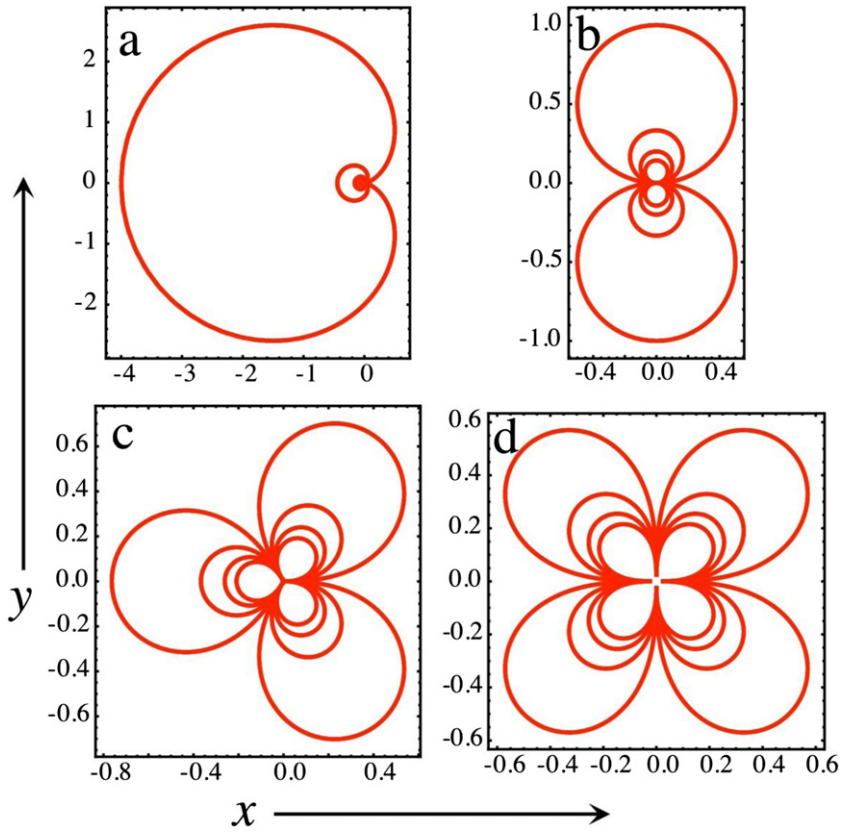

Figure 7. Trajectories $z_{n,m}(t)$ (equation (4.37)) for $c = -3.5(1)3.5$, for (a) $n = 3$, (b) $n = 4$, (c) $n = 5$, (d) $n = 6$.

The limiting behaviour of the high coefficients in the superposition is

$$c_{m,n,k} \underset{k\gg 1}{\to} 2^{m+n} k^{\frac{1}{2}(m+n)}. \tag{4.33}$$

To illustrate the convergence of the series (4.29), we consider the simplest case $m = n = 0$, for which the sequence of approximants is

$$\begin{aligned}\Psi_{0,0}(\mathbf{r}) &= \exp(-\mathrm{i}xy) \\ &= \lim_{K\to\infty} \sqrt{2}\ \exp\left(-\frac{1}{2}\left(x^2+y^2\right)\right) \sum_{k=0}^{K} \frac{(-\mathrm{i})^k}{2^k k!} H_k(x) H_k(y) \equiv \lim_{K\to\infty} \Psi_{K,0,0}(\mathbf{r}).\end{aligned} \tag{4.34}$$

Figure 5 shows how the approximants converge onto $\exp(-\mathrm{i}xy)$ around a circle $r = \sqrt{(x^2+y^2)}$.

Semiclassically, the relation between the states involves families of different trajectories with the same energy. According to (4.19), the trajectories (4.18) with complex energy E_c for

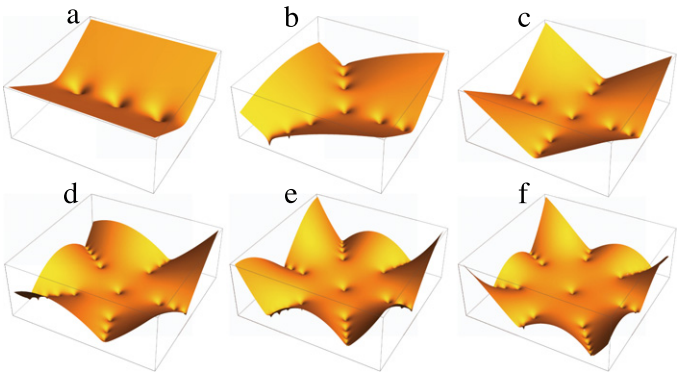

Figure 8. Log $\Psi_n(x,y)$ (equation (4.38)) for (a) $n = 0$, (b) $n = 1$, (c) $n = 2$, (d) $n = 3$, (e) $n = 4$, (f) $n = 5$.

given a must satisfy $A_- = \text{constant}/A_+$ for different values of A_+. For the complex modes (4.24) for a curl force ($a_2 \neq 0$), the trajectories form a family, illustrated in figure 6(a), of the escaping trajectories like that shown in figure 2. For a real, the trajectories are the familiar ellipses. A family, all with the same energy, is shown in figure 6(b); the trajectories have different eccentricities, with those more nearly circular being larger; this unfamiliar feature—contrasting with the standard SHO where the larger ellipses have more energy—originates in the negative signs of the y velocity and momentum in (2.4) and (2.5).

4.4. Power-law potential, zero energy

A general power-law potential is known to have intricate classical trajectories, and few exact results are known for the quantum counterpart. But for zero energy the trajectories and the quantum states can be described in some detail. A convenient form for this class of potentials is

$$U(z) = -2z^n. \tag{4.35}$$

The curl of the force $F(z) = -U'(z)$ is, from (2.1),

$$C(\boldsymbol{r}) = 4n(n-1)\, r^{n-2}\ \sin((n-2)\theta), \tag{4.36}$$

which is non-zero for $n > 2$, so these potentials describe complex curl forces.

In contrast to non-zero energies, for which almost all trajectories driven by curl forces escape, the zero-energy Newtonian trajectories are bounded: between $t = \pm\infty$, they trace closed loops. The exact solutions of (1.2) consist of branches, labelled by m:

$$z_{n,m}(t,c) = \frac{K_{n,m}}{(t-\mathrm{i}c)^{2/(n-2)}}, \quad K_{n,m} = \frac{\exp\left(2\pi \mathrm{i}m/(n-2)\right)}{(n-2)^{2/(n-2)}} \quad (0 \leqslant m \leqslant n-3). \tag{4.37}$$

Equation (2.3) confirms that the solutions have $E_c = 0$. The parameter c labels the different loops; a real parameter ic would simply correspond to changing the initial position on the loop. For different c, the loops are nested; some are shown in figure 7. The totality of loops for all real c fills the plane.

The quantum states can also be described analytically. The solutions of the complex-separated Schrödinger equations (3.4) with $E_X = E_Y = 0$ are Bessel functions [21], and the choice that

is nonsingular at $\boldsymbol{r}=0$ and singlevalued under continuation is

$$\begin{aligned}\Psi_n(\mathbf{r}) &= |\mathbf{r}|\, J_{1/(n+2)}\left(\frac{2}{n+2}(x+\mathrm{i}y)^{\frac{1}{2}n+1}\right) J_{1/(n+2)}\left(\frac{2}{n+2}(x-\mathrm{i}y)^{\frac{1}{2}n+1}\right)\\ &= r\left|J_{1/(n+2)}\left(\frac{2}{n+2}r^{\frac{1}{2}n+1}\ \exp\left(\mathrm{i}\left(\frac{1}{2}n+1\right)\theta\right)\right)\right|^2.\end{aligned} \tag{4.38}$$

These states are not square-integrable: they do not represent bound states. There are lines of zeros in the $n+2$ directions $\theta = 2m\pi/(n+2)$ $(0\leqslant m\leqslant n+1)$. Between these directions, $\Psi_n(\boldsymbol{r})$ grows exponentially with r. Figure 8 shows the first few cases. For $n=0$ (figure 8(a)), $U(z)$ is a constant potential, the Bessel functions $J_{1/2}$ are sines [21], and (4.38) is a zero-energy real superposition of complex plane waves (cf. section 4.1):

$$\Psi_0(\mathbf{r}) = \frac{1}{\pi}(\cosh\ 2y - \cos\ 2x)\,. \tag{4.39}$$

For $n=1$ (figure 8(b)), the Bessel functions $J_{1/3}$ can be expressed as a sum of the Airy functions Ai and Bi [21], so the zero-energy solutions (4.38) fall into the class considered in section 4.2, though different from the pure Ai states illustrated in figures 1(a) and 1(c). For $n=2$ (figure 8(c)), the Bessel functions $J_{1/4}$ are superpositions of parabolic cylinder functions $D_{-1/2}$ (4.21) [21] with $a=-4$ (cf (4.16) and (4.35)) and $E_X=E_Y=0$, different from the finite-energy solutions illustrated in figure 4.

Semiclassically, the large r asymptotics of the states $\Psi_n(\boldsymbol{r})$ should be expressible as a density $\rho(z)$of the family of trajectories $z_{n,m}(t,c)$ in (4.37) with a weight function $w(z(t,c))$. The relation, involving the unexpectedly simple Jacobian, is

$$\rho(z) = w(z)\left|\frac{\partial(x,y)}{\partial(t,c)}\right|^{-1} = \frac{w(z)}{4|z|^n}. \tag{4.40}$$

$w(z)$ is fixed by the asymptotics of $|\Psi_n(\boldsymbol{r})|^2$: narrow angular spikes in the growing sectors, contrasting sharply with the densities on individual trajectories.

5. Concluding remarks

The real Hamiltonian classical complex curl force interpretation explored here, and its Hermitian quantisation, can be applied to all potentials previously studied in complex dynamics. These include a range of potentials more sophisticated than linear and quadratic, where the classical trajectories have been understood in detail, including: cubic, quartic [26] and higher polynomial potentials; periodic potentials [8, 10, 27]; potentials with poles as well as zeros [11]; and multivalued potentials [6] (where trajectories can wander between the different Riemann sheets). In some cases [10], the classical dynamics can be described using elliptic functions, whose arguments as a function of time can pass close to poles, leading to periodic trajectories determined by arithmetic conditions, and wild excursions—erratic behaviour which although not chaotic in the usual sense (exponential separation of trajectories in a bounded region) is nevertheless sensitive to initial conditions. (Hamiltonians where the momentum p appears higher than quadratically [11] also generate very interesting complex-plane dynamics, but do not correspond to curl forces (1.1), because the resulting acceleration depends on velocity as well as position.)

The real classical Hamiltonians representing complex curl forces can all be quantised in the conventional way, using either of the Hermitian Hamiltonians in the Schrödinger

equations (3.1) or (3.2). Although formally conventional, the quantisation described here possesses unfamiliar features, raising a number of questions.

- Does nonconservativeness, implied by the nonzero curl (2.1), lead to characteristic quantum behaviour?
- What are the quantum implications of the anisotropic kinetic energy in (3.1)?
- For general quantised curl forces, where almost all classical trajectories are unbounded, is it possible to create solutions of (3.1) that for real energy grow slower than exponentially, e.g. polynomially, everywhere in the x, y plane? These would represent quantum states in the unbounded curl force potentials. They would be superpositions of the complex-separated states (3.3) with different energies E_X, E_Y, possibly complex but whose sum is real—complex-curl analogues of the non-curl superpositions (4.13) and (4.29); in the X, Y basis, they would be entangled.
- Can bound states exist, possibly associated with Bohr–Sommerfeld quantisation [26] of the isolated periodic orbits in cubic and higher potentials, even though almost all classical trajectories are unbounded? (In other contexts, for example scattering by rotationally symmetric potentials, isolated unstable closed orbits can exist; these are associated not with bound states, but with the interesting scattering phenomenon of 'orbiting' [28–30].)
- Can some of the bound states studied in PT non-Hermitian quantum mechanics [16] be alternatively understood as real-energy bound states of real Hamiltonians (3.1) in the full x, y plane, rather than in particular sectors?
- Does this study suggest an approach to the open question of quantising general classical curl forces, for which a Hamiltonian description seems unavailable [2]?

Although the emphasis of this paper has been mathematical—the exploration of some unusual classical and quantal formalisms—it is natural to consider applications. One possibility is that the anisotropic momentum dependence of the Hamiltonians considered here ((2.6) and (3.1)) could model the effects of external fields, represented by potentials satisfying Laplace's equation, on electrons in solids where an effective mass is negative, with confining walls modelled by boundary conditions (as in (4.7)).

Acknowledgments

I thank Professor E Abramochkin for help evaluating Airy integrals, and Professor P Shukla for a helpful comment.

Appendix A. Overlap integral (4.14) and superposition (4.13)

It is convenient to use the momentum representation:

$$\left\langle \psi\left(E_x,E_y\right)\middle|\,\Psi\left(E_X,E_Y\right)\right\rangle = \frac{1}{2\pi}\iint \mathrm{d}\mathbf{k}\left\langle \psi\left(E_x,E_y\right)\middle|\,\mathbf{k}\right\rangle\left\langle \mathbf{k}\middle|\,\Psi\left(E_X,E_Y\right)\right\rangle. \tag{A.1}$$

For $|\psi\rangle$ (cf (4.8)), this is derived from the integral representations of the two Ai functions, after scaling the integration variables:

$$\left\langle \psi\left(E_x,E_y\right)\middle|\,\mathbf{k}\right\rangle = \frac{1}{2\pi\sqrt{a_1a_2}}\,\exp\left(\mathrm{i}\left(-\frac{k_x^3}{6a_1}-\frac{k_y^3}{6a_2}+\frac{k_xE_x}{a_1}+\frac{k_yE_y}{a_2}\right)\right). \tag{A.2}$$

The counterpart for $|\Psi\rangle$ is, from (4.12),

$$\begin{aligned}\langle \mathbf{k} \,|\, \Psi\,(E_X,E_Y)\rangle &= \frac{1}{2\pi}\iint \mathrm{d}\mathbf{r}\ \exp\left(-\mathrm{i}\mathbf{k}\cdot\mathbf{r}\right)\langle \mathbf{r} \,|\, \Psi\,(E_X,E_Y)\rangle \\ &= \frac{1}{4\pi}\left(\frac{2}{|a|}\right)^{2/3} \\ &\quad\times\exp\left(\mathrm{i}\left(\frac{\left(k_x-\mathrm{i}k_y\right)^3}{12a}+\frac{\left(k_x+\mathrm{i}k_y\right)^3}{12a^*}\right)-\frac{E_X\,(x-\mathrm{i}y)}{a}\right)-\frac{E_Y\,(x+\mathrm{i}y)}{a^*}.\end{aligned} \tag{A.3}$$

This also uses the integral representations of $A\mathrm{i}$, and transformations of the double integral, using the convenient variables $K_X=(k_x-\mathrm{i}k_y)/2$, $K_Y=(k_x+\mathrm{i}k_y)/2$ (cf (2.7)), satisfying $\mathbf{k}\cdot\mathbf{r}=K_XX+K_YY$.

The overlap (A.1) now has the form

$$\left\langle \psi\left(E_x,E_y\right) \,\middle|\, \Psi\,(E_X,E_Y)\right\rangle = \frac{1}{8\pi^2\sqrt{a_1a_2}}\left(\frac{2}{|a|}\right)^{2/3}\iint \mathrm{d}\mathbf{k}\ \exp\left(\mathrm{i}\Phi\left(\mathbf{k}\right)\right), \tag{A.4}$$

in which $\Phi(\boldsymbol{k})$ is the sum of the two exponents in (A.2) and (A.3). After some algebra, and transformation to the new variables

$$q=k_xa_2+k_ya_1,\quad r=k_xa_1-k_ya_2, \tag{A.5}$$

with Jacobian $\left|\frac{\partial(q,r)}{\partial(k_x,k_y)}\right|=|a|^2$, the phase transforms to the degenerate cubic form

$$\begin{aligned}\Phi\left(\mathbf{k}\right) = &-\frac{q^3}{6|a|^2a_1a_2}+\frac{q}{|a|^2a_1a_2}\left(a_2^2E_x+a_1^2E_y+\mathrm{i}a_1a_2\left(E_X-E_Y\right)\right) \\ &+\frac{r}{|a|^2}\left(E_X+E_Y-\left(E_x-E_y\right)\right).\end{aligned} \tag{A.6}$$

The formula (4.14) now follows directly, with the Airy function coming from the q integration and the delta function from the r integration.

As a check on the formal manipulations leading to the overlap (4.14), we now confirm that the superposition (4.13) reproduces the complex-separated state (4.12) in position representation. After transforming the integration variables in (4.13) to

$$E_x=\frac{1}{2}E+v,\quad E_y=-\frac{1}{2}E+v \tag{A.7}$$

and the destination variables to

$$E_X=\frac{1}{2}E+u,\quad E_Y=\frac{1}{2}E-u, \tag{A.8}$$

and evaluating the E integration using the delta-function in (4.14), we need to show that

$$\begin{aligned}\left\langle \mathbf{r}\right|\left.\Psi\left(E_X,E_Y\right)\right\rangle = &\left(\frac{4}{a_1a_2}\right)^{1/3}\\ &\times\int_{-\infty}^{\infty}\mathrm{d}v\;\mathrm{Ai}\left((2a_1)^{1/3}\left(x-\frac{E+2v}{2a_1}\right)\right)\mathrm{Ai}\left((2a_2)^{1/3}\left(y-\frac{(-E+2v)}{a_2}\right)\right)\\ &\times\mathrm{Ai}\left(-\frac{2^{1/3}}{\left(|a|^2a_1a_2\right)^{2/3}}\left(\frac{1}{2}\left(a_2^2-a_1^2\right)E+|a|^2v+2\mathrm{i}a_1a_2u\right)\right).\end{aligned} \tag{A.9}$$

The integral has the form

$$L=\int_{-\infty}^{\infty}\mathrm{d}\xi\;\mathrm{Ai}\left(a\xi+b\right)\mathrm{Ai}\left(c\xi+d\right)\mathrm{Ai}\left(e\xi+f\right) \tag{A.10}$$

Its evaluation follows the treatment in section (3.6.3) of [26], but with a correction and slight modification suggested by Abramochkin (private communication); therefore it is worth stating the result explicitly.

$$L=\left|\frac{e}{f^{1/6}}\right|\mathrm{Ai}\left(\frac{\left(b-af/e\right)\delta-\left(c-af/e\right)\gamma}{K^{1/6}}\right)\mathrm{Ai}\left(\frac{\left(c-af/e\right)\alpha-\left(b-af/e\right)\beta}{K^{1/6}}\right), \tag{A.11}$$

involving the following quantities:

$$\begin{aligned}K&=\frac{1}{e^6}\left(a^6+c^6+e^6-2a^3c^3-2a^3e^3-2c^3e^3\right),\\ A&=1-\frac{a^3}{e^3},\quad B=-\frac{a^2c}{e^3},\quad C=-\frac{ac^2}{e^3},\quad D=1-\frac{c^3}{e^3},\\ \alpha^3&=\frac{1}{2}\left(A+\frac{1}{\sqrt{K}}\left(A^2D-3ABC+2B^3\right)\right),\\ \beta^3&=\frac{1}{2}\left(C-\frac{1}{\sqrt{K}}\left(AD^2-3BCD+2C^3\right)\right),\\ \gamma^3&=\frac{1}{2}\left(A-\frac{1}{\sqrt{K}}\left(A^2D-3ABC+2B^3\right)\right),\\ \delta^3&=\frac{1}{2}\left(C+\frac{1}{\sqrt{K}}\left(AD^2-3BCD+2C^3\right)\right).\end{aligned} \tag{A.12}$$

Explicitly, these quantities are

$$a=-\frac{2^{1/3}}{a_1^{2/3}},\quad b=\left(x-\frac{E}{2a_1}\right)(2a_1)^{1/3},\quad c=-\frac{2^{1/3}}{a_2^{2/3}},\quad d=\left(y+\frac{E}{2a_2}\right)(2a_2)^{1/3},$$
$$e=-\frac{2^{1/3}|a|^{2/3}}{(a_1a_2)^{2/3}},\quad f=-2^{1/3}\frac{\left(\frac{1}{2}\left(a_2^2-a_1^2\right)E+2\mathrm{i}a_1a_2u\right)}{(a_1a_2)^{2/3}\left|a^{4/3}\right|},$$
$$A=\frac{a_1^2}{|a|^2},\quad B=-\frac{a_1^{2/3}a_2^{4/3}}{|a|^2}\quad C=-\frac{a_1^{4/3}a_2^{2/3}}{|a|^2},\quad D=\frac{a_2^2}{|a|^2},\quad K=-\left(\frac{2a_1a_2}{|a|^2}\right)^2$$
$$\alpha=\left(\frac{a_1}{2a^*}\right)^{1/3},\quad \beta=\mathrm{i}\left(\frac{a_2}{2a^*}\right)^{1/3}\quad \gamma=\left(\frac{a_1}{2a}\right)^{1/3}\quad \delta=-\mathrm{i}\left(\frac{a_2}{2a}\right)^{1/3}. \tag{A.13}$$

Substitution into (A.11) leads to the expression (4.12) for $\langle \mathbf{r} \,|\, \Psi(E_X, E_Y)\rangle$, confirming the superposition.

ORCID iDs

M V Berry https://orcid.org/0000-0001-7921-2468

References

[1] Berry M V and Shukla P 2012 Classical dynamics with curl forces, and motion driven by time-dependent flux *J. Phys. A: Math. Theor.* **45** 305201
[2] Berry M V and Shukla P 2015 Hamiltonian curl forces *Proc. R. Soc.* A **471** 20150002
[3] Guha P 2020 Curl forces and their role in optics and ion trapping *Eur. Phys. J.* D **74** 99
[4] Berry M V and Shukla P 2016 Curl force dynamics: symmetries, chaos, and constants of motion *New J. Phys.* **18** 063018
[5] Bender C M and Boettcher S 1998 Real spectra in non-Hermitian Hamiltonians having **PT** symmetry *Phys. Rev. Lett.* **80** 5243–6
[6] Bender C M *et al* 2006 Classical trajectories for complex Hamiltonians *J. Phys. A: Math. Gen.* **39** 4219–38
[7] Bender C M, Holm D D and Hook D W 2007 Complexified dynamical systems *J. Phys. A: Math. Theor.* **40** F793–804
[8] Bender C M, Holm D D and Hook D W 2007 Complex trajectories of a simple pendulum *J. Phys. A: Math. Theor.* **40** F81–9
[9] Bender C M, Hook D W and Kooner K S 2010 Classical particle in a complex elliptic potential *J. Phys. A: Math. Theor.* **43** 165201
[10] Anderson A G and Bender C M 2012 Complex trajectories in a classical periodic potential *J. Phys. A: Math. Theor.* **45** 455101
[11] Bender C M and Hook D W 2014 Complex classical motion in potentials with poles and turning points *Stud. Appl. Math.* **133** 318–36
[12] Dynnikov I A and Novikov S P 2005 Topology of quasi-periodic functions on the plane *Russ. Math. Surv.* **60** 1–26
[13] Calogero F 1997 A class of integrable Hamiltonian systems whose solutions are (perhaps) all completely periodic *J. Math. Phys.* **38** 5711–9
[14] Grinevich P G and Santini P M 2007 Newtonian dynamics in the plane corresponding to straight and cyclic motions on the hyperelliptic curve μ^2 = ν^n − 1, $n = Z$: ergodicity, isochrony and fractals *Physica* D **232** 22–32
[15] Berry M V and Shukla P 2013 Physical curl forces: dipole dynamics near optical vortices *J. Phys. A: Math. Theor.* **46** 422001

[16] Bender C M 2007 Making sense of non-Hermitian Hamiltonians *Rep. Prog. Phys.* **70** 947–1018
[17] Gutzwiller M C 1973 The anistropic Kepler problem in two dimensions *J. Math. Phys.* **14** 139–52
[18] Gutzwiller M C 1990 *Chaos in Classical and Quantum Mechanics* (Berlin: Springer)
[19] Strocchi F 1966 Complex coordinates and quantum mechanics *Rev. Mod. Phys.* **38** 36–40
[20] Berry M V 1994 Evanescent and real waves in quantum billiards, and Gaussian beams *J. Phys. A: Math. Gen.* **27** L391–8
[21] Olver F W J *et al* (ed) 2010 *NIST Handbook of Mathematical Functions* (Cambridge: Cambridge University Press)
[22] Dingle R B 1973 *Asymptotic Expansions: Their Derivation and Interpretation* (New York: Academic)
[23] Vallée O and Soares M 2010 *Airy Functions and Applications to Physics* 2nd edn (London: Imperial College Press)
[24] Nanayakkara A 2004 Classical trajectories of 1D complex non-Hermitian Hamiltonian systems *J. Phys. A: Math. Gen.* **37** 4321–44
[25] Abramowitz M and Stegun I A 1972 *Handbook of Mathematical Functions* (Washington, DC: National Bureau of Standards)
[26] Anderson A G, Bender C M and Morone U I 2011 Periodic orbits for classical particles having complex energy *Phys. Lett.* A **375** 3399–404
[27] Arpornthip T and Bender C M 2009 Conduction bands in classical periodic potentials *Pramana* **73** 259–67
[28] Ford K W and Wheeler J A 1959 Semiclassical description of scattering *Ann. Phys., NY* **7** 259–86
[29] Ford K W and Wheeler J A 1959 Application of semiclassical scattering analysis *Ann. Phys., NY* **7** 287–322
[30] Tabor M 1977 Fast oscillations in the semiclassical limit of the total cross section *J. Phys. B: At. Mol. Phys.* **10** 2649–62